Plasmonics (2024) 19:395–401
https://doi.org/10.1007/s11468-023-01973-z

RESEARCH

Highly Confined Terahertz Surface Plasmons Generation in Graphene-Coated Optical Fiber by Nonlinear Mixing of Two Laser Beams

Neha Verma[1] · Anil Govindan[1] · Pawan Kumar[2,3]

Received: 23 May 2023 / Accepted: 24 July 2023 / Published online: 18 August 2023

Abstract

Graphene is a most suitable 2D material for Terahertz surface plasmons generation (THz-SPs). An efficient mechanism of THz SPs generation in graphene-coated optical fiber is proposed. The thickness of the graphene sheet and radius of an optical fiber are important parameters to influence the THz SPs resonant frequency. Two lasers exert a ponderomotive force at difference frequency on the electrons in graphene and it induces a nonlinear current which driving the THz SPs. The normalized amplitude of graphene THz SPs decreases with frequency because the nonlinear coupling gets weaker. This scheme will be useful making the compact THz GPs source, THz plasmon sensors, and would be useful for making the graphene cylindrical waveguide have applications in various disciplines of science and medical science.

Keywords Surface plasmons · Graphene-coated optical fiber · Laser beams

Introduction

There is a substantial interest of terahertz radiation generation due to its wide applications in outer space communications, biomedical imaging, tomography, precision radar, and other areas [1–7]. Due to the lack of efficient sources and detectors in THz range or so-called THz gap (0.1–10THz), however, this THz gap still remains a challenge for modern technology and poses significant limitations for further developments in this field and these limitations, arising due to the nature of light/material interaction at THz frequencies.

The laser-based THz radiation generation sources are attractive due to relative simplicity and suitability for modest THz power [8, 9]. The short pulse laser–semiconductor interactions produce the THz radiation by modulation of transient dc current in photoconductors [10, 11]. Intense short pulse laser plasma interaction also offers potential schemes [12–15] for the generation of long pulse and high power THz, required for THz communication, remote sensing, and ultrafast material characterization.

Highly confined guided electromagnetic waves are used as a probing radiation and having large number of applications [16–24], known as surface plasmons (SPs). SPs are guided electromagnetic modes propagate along the interface between a conductor and a dielectric or conductor and air with their field amplitude falling off exponentially away from it in either medium [25–27]. The structured surfaces that also support SPs at THz frequency range are called designer plasmonic structures or "spoof" SP structures [28–30]. Two structures, an ultrathin metal film dielectric substrate and a metal-coated optical fiber, are shown to support the low loss THz SPs with weak attenuation [31, 32].

Graphene is a 2D material, which has unique properties and potential applications for making the nano devices [33–40]. The most striking feature of graphene is that all its Dirac electrons have the same speed, as energy versus momentum relation is linear, irrespective of their energy. In graphene, the localized electron motion in a plane with very small electron effective mass giving rise to high in-plane conductivity. The two-dimensional nature of graphene also supports plasmons with wavelengths substantially smaller than free-space electromagnetic radiation of the same frequency by approximately two orders of magnitude and generating large non-local effects. Graphene plasmons (GPs)

✉ Pawan Kumar
kumarpawan_30@yahoo.co.in

[1] Department of Physics, MMH College Ghaziabad, UP, India

[2] Department of Physics, Raj Kumar Goel Institute of Technology, Ghaziabad UP-201003, India

[3] Research Centre for Compact Radiation Sources, Raj Kumar Goel Institute of Technology Ghaziabad, U.P 201003, India

are used for making the compact radiation sources on chip in infrared–visible–ultraviolet range [41].

The difference frequency generation (DFG) at mid-infrared is enhanced due to the presence of plasmons resonance [42–45]. The graphene holds a great promise for designing the plasmonic sensors or new THz sources. An all-optical coupling scheme is used for plasmon generation in graphene. An electron beam is used for coherent and tunable THz radiation generation from multilayer graphene deposited on a substrate [46]. Despite the recent intensive research, generation of coherent and tunable THz radiation remains a significant challenge. Graphene-coated dielectric nanowire (GNW) supports the Eigen GPs [47]. These modes are depending on the nanowire radius, nanowire permittivity, and chemical potential of graphene that are studied as well; the radius of optical fiber has a strong impact on the modal behavior in graphene-coated optical fiber, such as the number of supported mode. Montasir Qasymeh proposed a THz plasmonic waveguide in frequency range 1–10 THz, which is based on metal–insulator-metal nanostructure filled with optical nonlinear material lithium niobate [48]. Montasir Qasymeh proposed a THz waveguide that is designed to confine a single THz mode having a novel nanostructure comprising graphene parallel plates filled with lithium niobate (i.e., LiNbO3) crystal [49, 50].

In this paper, we put forth the new and efficient scheme of THz GPs generation via the nonlinear mixing of two laser beams in the graphene-coated optical fiber. The fiber has a dielectric ripple (volume grating) of wave number q. The ripple imparts spatial harmonics to lasers shifted by q. The lasers and their spatial harmonics exert a difference frequency ponderomotive force on film electrons with wave number $k_z = k_{1z} - k_{2z} + q$, where k_{1z} and k_{2z} are the wave numbers of the lasers. Two lasers exert a ponderomotive force at difference frequency on the electrons in graphene and it induces a nonlinear current which driving the THz SPs. Our calculations and approach in this manuscript are based on single mode propagation optical fiber.

In the "THz Graphene Plasmons in Graphene-Coated Optical Fiber" section, we developed the formalism of THz GPs in graphene-coated fiber and the nonlinear mixing of lasers and THz excitation is discussed in the "THz Surface Plasmons Generation in Graphene-Coated Optical Fiber by Nonlinear Mixing of Two Laser Beams" section. We discussed the results in the "Conclusion" section.

THz Graphene Plasmons in Graphene-Coated Optical Fiber

Consider an optical fiber (cf.1) of radius "a" is coated by graphene sheet of conductivity σ_g Consider the thin film of graphene is a layer zero thickness and infinite conductivity and the current density in graphene layer may be defined as:

$$J = \sigma_g d\delta(r-a)E_z\big|_{r=a}\hat{z} = \sigma_g dE_z\big|_{r=a}\hat{z}. \tag{1}$$

The graphene plasmons (GPs) propagate along $\hat{z}$ direction of fiber, i.e., length of fiber with variation as $exp\left[-i\left(\omega t - k_z z\right)\right]$ is shown in Fig. 1. The electric and magnetic fields of the GPs in different regions can be written as for $r < a$(glass) region 1:

$$\begin{aligned} E_{1z} &= A_{01}I_0\left(\alpha_1 r\right) exp\left[-i\left(\omega_1 t - k_{1z}z\right)\right], \\ H_{1\varphi} &= \frac{\omega\varepsilon_0\varepsilon_1}{i\alpha_1} A_{01}I_0'\left(\alpha_1 r\right) exp\left[-i\left(\omega_1 t - k_{1z}z\right)\right], \end{aligned} \tag{2}$$

where $\alpha_1^2 = k_z^2 - \frac{\omega^2}{c^2}\varepsilon_1$. For region $r > a$ (vacuum) region 2, the electric and magnetic fields of the GPs are:

$$\begin{aligned} E_{2Z} &= A_{02}K_0\left(\alpha_2 r\right) exp\left[-i\left(\omega_2 t - k_{2z}z\right)\right], \\ H_{2\varphi} &= -\frac{\omega\varepsilon_0\varepsilon_2}{i\alpha_2} A_{02}K_0'\left(\alpha_2 r\right) exp\left[-i\left(\omega_2 t - k_{2z}z\right)\right], \end{aligned} \tag{3}$$

where $a_2^2 = k_z^2 - \frac{\omega^2}{c^2}\varepsilon_2$. Using jump condition on $\vec{H}$ (at $r > a$):

$$\vec{H}_\phi\,|_2 - \vec{H}_\phi\,|_1 = \sigma_g dE_z\,|_{r-a}, \tag{4}$$

Putting the Eqs. (2) and (3) into Eq. (4), one may get:

$$\frac{\varepsilon_2}{a_2}\frac{K_0'(\alpha_2 a)}{K_0(\alpha_2 a)} - \frac{\varepsilon_1}{a_1}\frac{I_0'(\alpha_2 a)}{I_0(\alpha_2 a)} = -\frac{i\sigma_g d}{\omega\varepsilon_0}. \tag{5}$$

A similar dispersion relation is derived for Eigen GP modes in graphene-coated dielectric nanowire (GNW) which are proposed by solving the Maxwell equations in cylindrical coordinate [47]. In Fig. 2, we have plotted the normalized frequency ω/ω_p versus normalized wave vector $k_z c/\omega_p$ for two normalized radii $a\omega_p/c = 10^{-2}, a\omega_p/c = 10^{-3}$ of optical fiber, normalized graphene sheet thickness $d\omega_p/c = 0.08$. The figure shows that with increasing the radius of optical fiber, the coupling is between lasers and graphene plasmons become weak. As the frequency increases with wave number, however, the phase velocity of graphene plasmons slows down with increasing the frequency. The graphene-coated microfiber Bragg grating (GMFBG) is using gas sensing

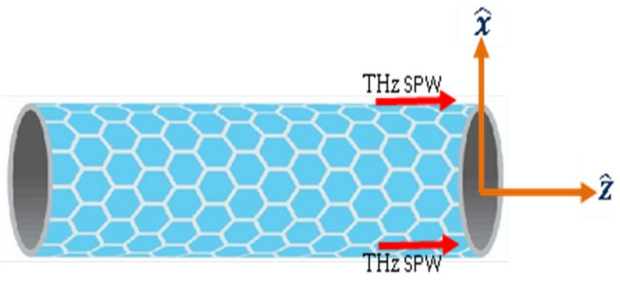

Fig. 1 THz GPs propagation in graphene-coated optical fiber

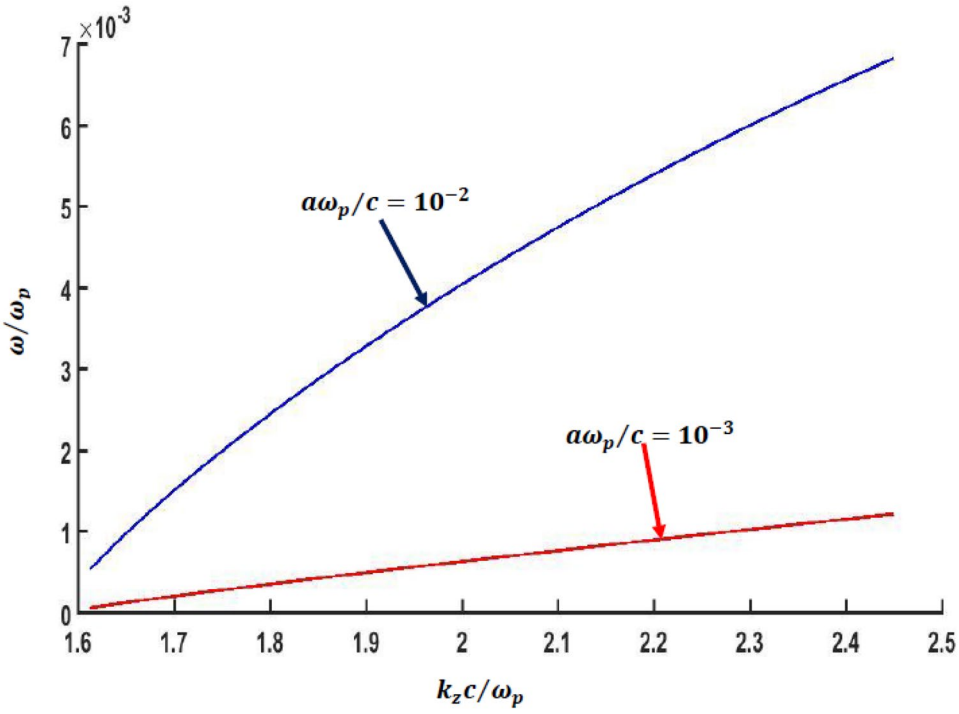

Fig. 2 Dispersion relation of graphene plasmons

which is reported by Yu Wu et al. [51]. There is surface field enhancement and gas absorption of a GMFBG. In graphene-coated optical fiber, the confinement of modes is very high, so it has high sensitivity.

THz Surface Plasmons Generation in Graphene-Coated Optical Fiber by Nonlinear Mixing of Two Laser Beams

Let two laser beams are propagated in the azimuthally symmetric mode inside the graphene-coated fiber (Fig. 2). The electric fields of the laser beams inside the fiber are:

$$\vec{E}_1 = A_1\left[\hat{z}J_0\left(k_{1\perp}r\right) + i\hat{r}\frac{k_{1z}}{k_{1\perp}}J_0'\left(k_{1\perp}r\right)\right] exp\left[-i\left(\omega_1 t - k_{1z}z\right)\right]. \tag{6}$$

$$\vec{E}_2 = A_2\left[\hat{z}J_0\left(k_{2\perp}r\right) + i\hat{r}\frac{k_{2z}}{k_{2\perp}}J_0'\left(k_{2\perp}r\right)\right] exp\left[-i\left(\omega_2 t - k_{2z}z\right)\right]. \tag{7}$$

The core of fiber to have a dielectric constant ripple for phase matching condition is:

$$\varepsilon_g = \varepsilon_{g0} + \varepsilon_{gq}\,,\ \varepsilon_{gq} = \varepsilon_{g2}e^{iqz}. \tag{8}$$

The displacement vector inside the fiber is $\vec{D}_1 = \varepsilon_g\vec{E}_1 = \varepsilon_{g0}\vec{E}_1 + \frac{1}{2}\varepsilon_{gq}\vec{E}$ and acquires a component that goes as $e^{-i[\omega_1 t-(k_{1z}+q)z]}$. This component produces an electromagnetic field (in compliance with $\nabla.\vec{D} = 0$):

$$\vec{E}_{1+} \cong -\frac{\varepsilon_{gq}}{2\varepsilon_{g0}}\vec{E}_1 \approx exp\left[-i\left\{\omega_1 t - \left(k_{1z}+q_z\right)z\right\}\right]. \tag{9}$$

Similarly:

$$\vec{E}_{2+} \cong -\frac{\varepsilon_{gq}}{2\varepsilon_{g0}}\vec{E}_2 \approx exp\left[-i\left\{\omega_2 t - \left(k_{2z}+q_z\right)z\right\}\right]. \tag{10}$$

Here, the phase matching conditions demands that:

$$\omega_{SPTHz} = \omega_1 - \omega_2\,,\ k_{SPTHz} = k_{1z} - k_{2z} + q. \tag{11}$$

The lasers impart oscillatory velocities to the electrons, given as:

$$\vec{v}_{1+} = \frac{\vec{E}_{1+}}{mi\omega_1},\ \rightarrow \vec{v}_{2+} = \frac{e\vec{E}_{2+}}{mi\omega_2}. \tag{12}$$

These laser beams also impart the ponderomotive force F_{pz} on electrons at beat frequency given by:

$$F_{pz} \approx \frac{mi\left(k_{1z} - k_{2z} + q\right)}{2}\vec{v}_1\vec{v}_2^{*}\frac{\varepsilon_{gq}}{2\varepsilon_{g0}}. \tag{13}$$

This ponderomotive force also imparts oscillatory velocity to electrons at frequency $\left(\omega_1 - \omega_2\right)$ and may be written as:

$$\vec{v}_\omega - = \frac{\hat{z}F_{pz}}{im\omega}, \tag{14}$$

>and nonlinear current in graphene sheet may be written as:

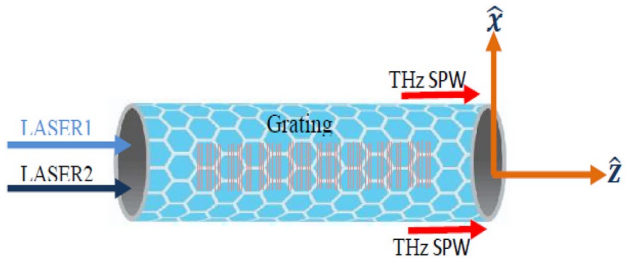

Fig. 3 THz GPs excitation via nonlinear mixing of lasers in graphene-coated optical fiber

$$\vec{J}_{\omega}^{NL} = \hat{Z}\frac{n_0 e\left(k_{1z} - k_{2z} + q\right)}{2\omega}\vec{v}_1\vec{v}_2^{*}\frac{\varepsilon_{gq}}{2\varepsilon_{g0}} \cong \hat{z}Fd\delta\,(r)\,exp\left[-i\left(\omega_{SP}t - k_{SP}z\right)\right]. \tag{15}$$

where:

$$\vec{F} = \frac{n_0 e k_{sp}}{4\omega}\frac{e^2 \mid E_1 \mid\mid E_2 \mid}{m^2\,\omega_1\,\omega_2}\frac{\varepsilon_{gq}}{\varepsilon_{g0}}\,. \tag{16}$$

This nonlinear current density is localized in graphene sheet, which is the source of THz radiation graphene plasmons. The electric and magnetic field vectors for GPs are given Fig. 3 as:

For $r < a$ (glass):

$$\vec{E}_1 = A_1\left[\hat{z}I_0(\alpha_1 r) - i\hat{r}\frac{k_z}{a_1}I_0'(\alpha_1 r)\right]exp\left[-i(\omega_1 t - k_1 z)\right],$$
$$\vec{H}_{\phi} = \frac{i\omega\varepsilon_0\varepsilon_1}{\alpha_1}A_1 I_0'(\alpha_1 r)\,exp\left[-i(\omega_1 t - k_1 z)\right]\cdot \tag{17}$$

For $r > a$ (vacuum), the electric and magnetic field vectors for GPs are given as:

$$\vec{E}_2 = A_2\left[\hat{z}K_0(\alpha_2 r) - i\hat{r}\frac{k_z}{a_2}K_0'(\alpha_2 r)\right]exp\left[-i(\omega_2 t - k_2 z)\right],$$
$$\vec{H}_{\phi} = \frac{i\omega\varepsilon_0}{\alpha_2}A_2 K_0'(\alpha_2 r)\,exp\left[-i(\omega_2 t - k_2 z)\right]\cdot \tag{18}$$

The jump condition on the $\overrightarrow{H_{\phi}}$ component of the GPs at $r = a$ gives:

$$DA_0 = \frac{-i\,Fd\,/\,\omega\varepsilon_0}{K_0'(\alpha_2 a)}, \tag{19}$$

where:

$$D = \frac{\varepsilon_1}{\alpha_1}\frac{I_0'(\alpha_1 a)}{I_0(\alpha_1 a)} - \frac{1}{a_2}\frac{K_0'(\alpha_1 a)}{K_0(\alpha_1 a)} - \frac{\sigma_g d}{i\omega\varepsilon_0}. \tag{20}$$

Solving Eq. (19), it yields the amplitude of THz GPs:

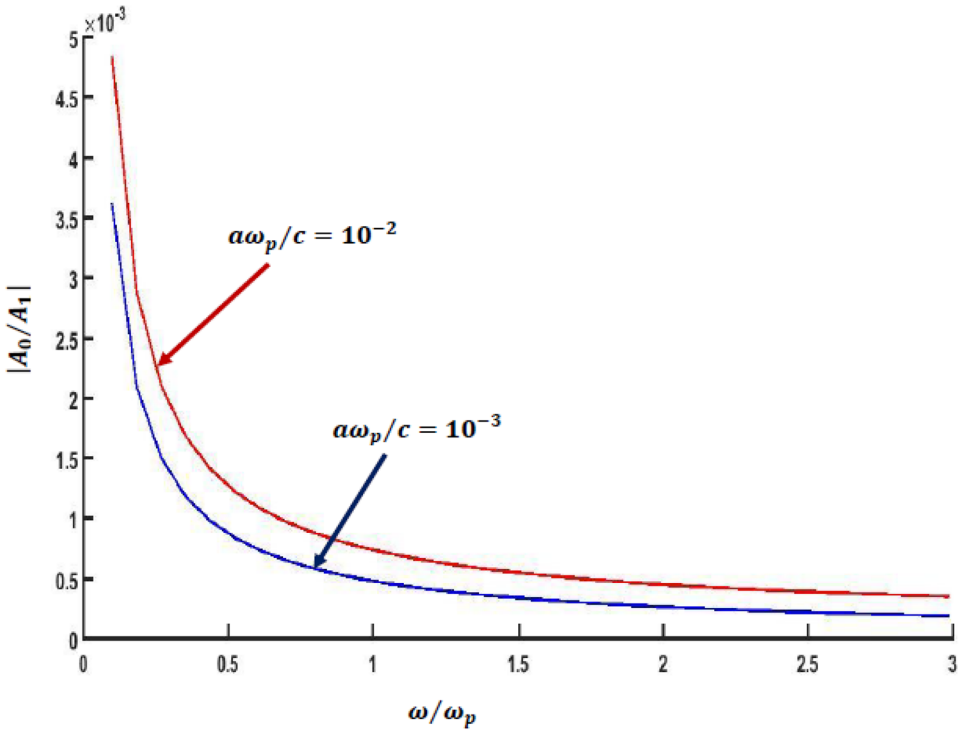

Fig. 4 Normalized THz graphene surface plasmons amplitude variation with normalized frequency for different two different normalized radii of optical fiber and fixed thickness of graphene sheet

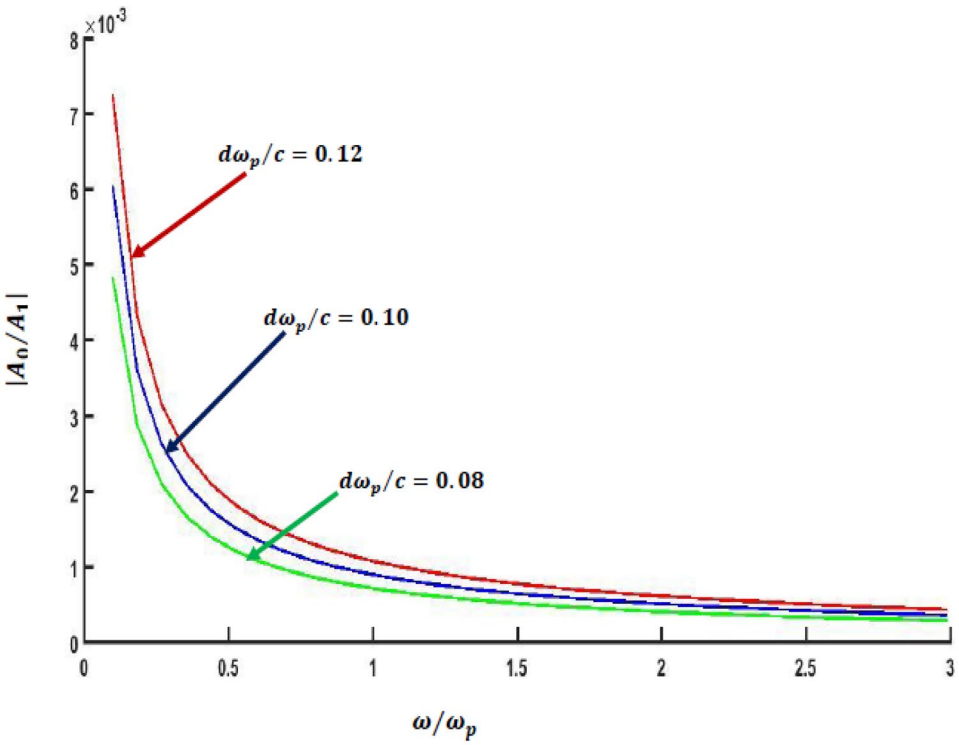

Fig. 5 Normalized THz graphene surface plasmons amplitude variation with normalized frequency for different normalized thickness of graphene sheet and fixed normalized radius of optical fiber

$$A_0 = \frac{FdL/\omega\varepsilon_0}{K_0'(\alpha_2 a)\partial D/\partial k_{sp}}. \tag{21}$$

At exact phase matching condition, D is vanishing. However, due to finite length of interaction $L = 2r_0$ where r_0 is laser spot size, so D can be replaced by region $D \cong -i\left(\partial D/\partial k_z\right)\left(\partial/\partial_z\right)$, Eq. (19) can be written as:

$$\frac{\partial D}{\partial k_z} = -k_z\left[\frac{\varepsilon_1}{\alpha_1^3}\frac{I_0'(\alpha_1 a)}{I_0(\alpha_1 a)} - \frac{1}{\alpha_1^3}\frac{K_0'(\alpha_2 a)}{K_0(a_2 a)}\right]. \tag{22}$$

Solving and rearranging the terms in Eq. (22), we have the normalized amplitude of THz graphene plasmons:

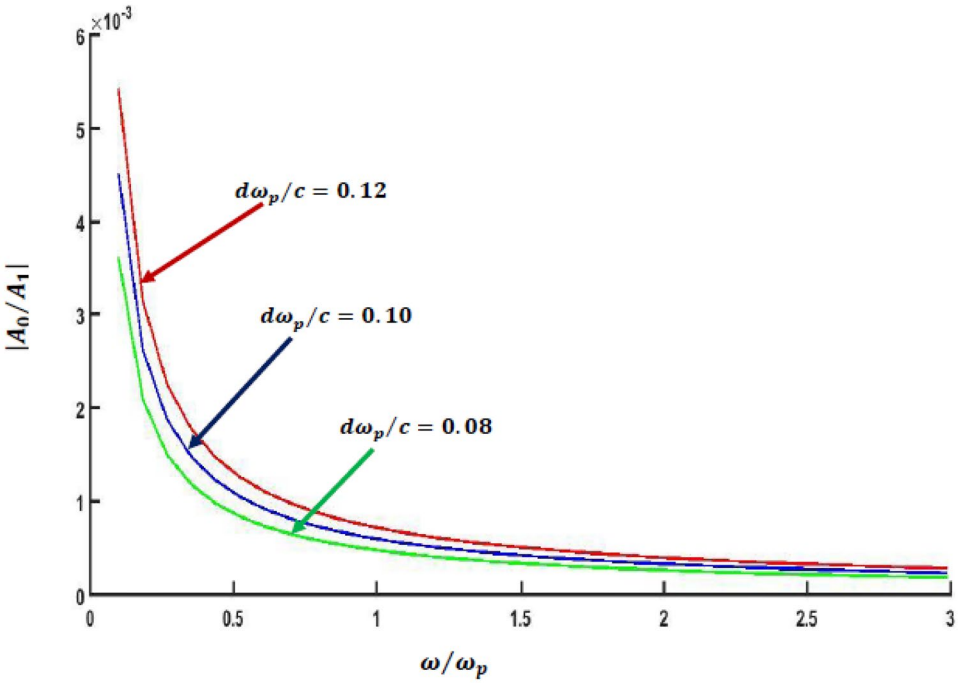

Fig. 6 Normalized THz graphene surface plasmons amplitude variation with normalized frequency for different normalized thickness of graphene sheet and fixed normalized radius of optical fiber

$$\left|\frac{A_0}{A_1}\right| = \frac{1/(\omega/\omega_P)(\omega/4\omega_1)(k_{SP}/k_z)(|v_2|/c)(\varepsilon_{gq}/\varepsilon_{g0})(d\omega_p/c)(L\omega/c)}{K_0'(\alpha_0 a)\left(\frac{\varepsilon_1}{(k_z^2-(\omega^2/c)\varepsilon_1)^{3/2}}\frac{I_0'(\alpha_1 a)}{I_0(\alpha_1 a)} - \frac{1}{(\omega^2/c)^{3/2}}\frac{K_0'(\alpha_2 a)}{K_0(\alpha_2 a)}\right)}. \quad (23)$$

Equation (23) gives the amplitude of terahertz graphene plasmon. For following parameters: $v_2 = 10^6 m/s$; $c = 3 \times 10^8 m/s$; $\omega = 10^{13}\ rad/s$; $k_z^2 c^2/\omega^2 = 2.6$; $\omega_1 = 2\times 10^{12} rad/s$; $\omega_p \approx 2.5 \times 10^{12} rad/s$, normalized thickness $d\omega_p/c = 0.08, 0.10, 0.12$, normalized radius of optical fiber $a\omega_p/c = 10^{-2}, 10^{-3}$ $L\omega/c = 10^3$, $\varepsilon_{g0} = 0.2$. For CO_2 laser, $e|E_2|/m\omega_2 c = 10^{-2}$, corresponds to an intensity $3\times 10^{12} W/cm^2$ and power ~ 8 MW. For $1\,\mu m$ wavelength, it corresponds to an intensity of $3\times 10^{12} W/cm^2$. Figures 4, 5, and 6 show that as the frequency raises, the normalized amplitude of THz SPW decreases. It is due to the weakening of the nonlinear coupling of SPs at higher frequencies.

Conclusion

In conclusion, the graphene-coated fiber offers the promise of producing phase-matched THz graphene plasmons using laser moderate power (MW range) and intensity. The nonlinearity arises through the ponderomotive force and phase matching is provided by the volume grating of suitable wave number inside the fiber. The efficiency is one order of magnitude smaller than the ideal efficiency given by Manley Rowe relations. The thickness of the graphene sheet and radius of an optical fiber are important parameters to influence the THz graphene surface plasmons resonant frequency. The normalized amplitude of THz GPS decrease with frequency as the nonlinear coupling gets weaker. The fiber configuration is more suitable as the grating structures in optical fibers are routinely available. The efficiency of the device is around 0.01% at a laser intensity of 3×10^{14} W/cm^2.

Author Contribution All authors Neha Verma, Anil Govindan, and Pawan Kumar contributed equally to this work.

Data Availability The data that supports the findings of this study are available within the article.

Code Availability Not applicable.

Declarations

Ethics Approval Not applicable.

Consent to Participate Not applicable.

Consent for Publication Not applicable.

Conflict of Interest The authors declare no competing interests.

References

1. Ferguson B, Zhang X-C (2002) Nat Mater 1:26
2. Huber R, Tauser F, Brodschelm A, Bichler M, Abstreiter G, Leitenstorfer A (2001) Nature 414:286
3. Nagel M, Brucherseifer M, Bolivar PH, Kurz H, Bosserhoff A, Buttner R (2002) Appl Phys Lett Appl Phys Lett 80:154
4. Grischkowsky D, Søren Keiding, Martin van Exter, Ch Fattinger J (2006) Opt Soc Am B 7:(1990)
5. Mittleman DM, Jacobsen RH, Nuss MC (1996) IEEE. J Selected Topics in Quantum Electronics 2:679
6. Beard MC, Turner GM, Schmuttenmaer CA (2001) J Appl Phys 90:5915
7. Federici J, Moeller L, Shen YC, Lo T, Taday PF, Cole BE, Tribe WR, Kemp MC (2005) Appl Phys Lett 86:241116
8. Spangle P, Penano JR, Hafizi B, Kapetanakas CA (2004) Phy Rev E 69:066415
9. Zhao J. Zhang Y, Wang Z, Chu W, Zeng B, Liu YZ, Cheng Xu (2014) Laser Phys Lett 11:095302
10. Cicėnas P, Geižutis A, Malevich VL, Krotkus A (2015) Opt Letts 40:(22)5164
11. Zhang X-C, Jin Y, Kingsley LE, Weiner M (1993) Appl Phys Lett 62:2477
12. Hamster H, Sullivan A, Gordon S, White W, Falcone RW (1993) Phys Rev Lett 71:2725
13. Antonsen Jr TM, Palastro J, Howard Milchberg M (2007) Phys Plasmas 14:033107
14. Xu Xie, Jingzhou Xu, Jianming Dai, Zhang X-C (2007) Appl Phys Lett 90:141104
15. Cook DJ, Hochstrasser RM (2000) Opt Lett 25:1210
16. Ozbay E (2006) Science 311:189
17. Barnes Dereux A, Ebbesen TW (2003) Nature 424:824
18. Liu H, Lee Y, Xiong C (2007) Sun and X. Zhang, Science 315:1686
19. Kim S, Jin J, Kim Y-J, Park I-Y, Kim Y, Kim SW (2008) Nature 453:757
20. Bozhevolnyi I, Volkov VS, Devaux E, Laluet J-Y, Ebbesen TW (2006) Nature 440:508
21. Kumar P, Tripathi VK, Liu CS (2008) J Appl Phys 104:033306
22. Bergman DJ, Stockman MI (2003) Phys Rev Lett 90:027402
23. Catchpole KR, Polman A (2008) Opt Express 16:21793
24. Homola Yee SS, Gauglitz G (1999) Sens Actuators B 54(3)
25. Raether H (1988) Surface Plasmons on Smooth and Rough Surfaces and on Gratings. Springer, Berlin
26. Boardman D (1982) Electromagnetic Surface Modes. Wiley, New York
27. Maier SA (2007) Plasmonics: Fundamentals and Applications. Springer-Verlag, New York
28. Pendry JB, Martin-Moreno L, Garcia-Vidal FJ (2004) Science 305:847
29. Garcia-Vidal FJ, Martin-Moreno L, Pendry JB (2005) J Opt A: Pure Appl Opt 7:S97
30. Williams CR, Andrews SR, Maier SA, Fernandez-Domınguez AI, Martın-Moreno L, Garcıa-Vidal FJ (2008) Nature Photon 2:175
31. Pawan Kumar VK, Tripathi (2013) J Appl Phys 114:053101
32. Pawan Kumar, Tripathi VK (2013) Opt Lett 38(18):3475
33. Novoselov KS, Geim AK, Morozov SV, Jiang D, Katsnelson MI, Grigorieva IV, Dubonos SV, Firsov AA (2005) Nature 438:197
34. Zhang Y, Tan Y-W, Stormer HL, Kim P (2005) Nature 438:201
35. Geim AK (2009) Science 324:1530
36. Basov DN, Fogler MM, Lanzara A, Wang F, Zhang Y (2014) Rev Modern Phys 86:959
37. Geim AK, Novoselov KS (2007) Nat Mater 6:183
38. Wallace PR (1947) Phys Rev 71:622
39. Castro Neto AH, Guinea F, Peres NMR, Novoselov KS, Geim AK (2009) Rev Mod Phys 81:109

40. Grigorenko AN, Palini M, Novoselov KS (2012) Nat Photonics 6:749
41. Wong LJ, Kaminer I, Ilic O, Joannopoulos JD, Soljačić M (2016) Nat Photonics 10:46
42. Constant TJ, Hornett SM, Chang DE, Hendry E (2015) Nat Phys 12:124
43. Yao B, Liu Y, Huang S-W, Choi C, Xie Z, Flores JF, Wu Y, Yu M, Kwong D-L, Huang Y, Rao Y, Duan X, Wong CW (2018) Nat Photon 12:22
44. Yao XH, Tokman M, Belyanin A (2014) Phys Rev Lett 112:055501
45. Neha Verma, Anil Govindan and Pawan Kumar (2020) Plasmonics 15(6)
46. Liu S, Zhang C, Hu M, Chen X, Zhang P, Gong S, Zhao T, Zhong R (2014) Appl Phys Lett 104:201104
47. Yixiao Gao, Guobin Ren, Bofeng Zhu, Huaiqing Liu, Yudong Lian, Shuisheng Jian (2014) Optics Express 22(20):24322
48. Qasymeh M (2016) IEEE J Quantum Electron 52(4):8500207
49. Qasymeh M (2017) IEEE/OSA Journal of Lightwave Technology 35(9):1654
50. Qasymeh M (2012) International Journal of Optics 2012:486
51. Yu Wu, Baicheng Yao, Anqi Zhang, Yunjiang Rao, Zegao Wang, Yang Cheng, Yuan Gong, Weili Zhang, Yuanfu Chen, Chiang KS (2014) Optics Letters 39(5):1235